

The Analysis of Correction Effect of Motion Artifacts in PET Images Using Respiratory Gating System

Jinyoung Kim, Gyehwan Jin

Received: 6 September 2022 / Accepted: 30 November 2022 / Published online: 30 December 2022

©The Author(s) 2022

Abstract– PET is used effectively for biochemical or pathological phenomena, disease diagnosis, prognosis determination after treatment, and treatment planning because it can quantify physiological indicators in the human body by imaging the distribution of various biochemical substances. However, since respiratory motion artifacts may occur due to the movement of the diaphragm due to breathing, we would like to evaluate the practical effect by using the a device-less data-driven gated technique called Motion Free (DDG) with the phase-based gating correction method called Q.static scan mode. In this study, images of changes in moving distance (0 cm, 1 cm, 2 cm, 3 cm) and degree of slope (0°, 2.5°, 5°, 10°) were acquired using a breathing-simulated moving phantom. The diameters of the six spheres in the phantom are 10 mm, 13 mm, 17 mm, 22 mm, 28 mm, and 37 mm, respectively. According to SUV_{max} and SUV_{mean} measurements, when DDG was applied based on the moving distance,

the average SUV_{max} of the correction effect by the moving distance was improved by 1.92, 2.48, 3.23 and 3.00, respectively, and the average SUV_{mean} was improved by 0.04, 0.72, 1.36 and 1.49, respectively.

When DDG was applied based on the diameter of the phantom spheres, the average SUV_{max} of the correction effect by the moving distance was improved by 2.37, 2.02, 1.44, 1.20, 0.42 and 0.52, and the average SUV_{mean} was improved by 1.36, 1.23, 0.99, 0.82, 0.57 and 0.43, respectively. The correction effect by the degree of slope also improved the average SUV_{max} when DDG was applied to 2.93, 2.87, 1.61 and 1.45 respectively, and the average SUV_{mean} to 1.61, 1.27, 0.8 and 0.95 respectively, based on the degree of slope. when DDG was applied based on the diameter of the phantom sphere, the average SUV_{max} was improved by 0.77, 1.73, 1.84, 2.56, 3.46 and 2.93 respectively and the average SUV_{mean} was improved by 0.56, 0.44, 1.19, 0.98, 1.66 and 2.13, respectively. In the visual comparison due to the change of the moving distance and the degree of slope, it was found that the more the moving distance increases, the greater the degree of slope increases, the greater the correction effect of DDG. In the case of the area ratio, Based on the image with a moving distance of 0 cm, when moving distance was 1 cm, 2 cm and 3 cm, the difference between applying and not applying DDG was 5%, 12%, and 18%, respectively. Based on an image with degree of slope of 0°, when degree of slope was 2.5°, 5° and 10°, the difference between applying and not applying DDG was 6%, 7%, and

Jinyoung Kim

Dept. of Nuclear Medicine, Chungbuk University Hospital

e-mail : korotkoff@khidi.or.kr

Gyehwan Jin (✉) **corresponding author**

Dept. of Radiology, Nambu University

e-mail : ghjin@nambu.ac.kr

7%, respectively. In the case of the average density ratio, Based on an image with a moving distance of 0 cm, when moving distance was 1 cm, 2 cm and 3 cm, the difference between applying and not applying DDG was 3%, 6%, and 8%, respectively. Based on an image with degree of slope of 0°, when degree of slope was 2.5°, 5° and 10°, the difference between applying and not applying DDG was 3%, 4%, and 5%, respectively. In the comparison of FWM, FWHM, and FWTM, Based on the image with a moving distance of 0 cm, when moving distance was 1 cm, 2 cm and 3 cm, the difference between applying and not applying DDG was 1.6%, 9% and 9.4% in FWM, 4.4%, 7.6% and 6.4% in FWHM, 12.1%, 23.4% and 30.5% in FWTM respectively. Based on an image with degree of slope of 0°, when degree of slope was 2.5°, 5° and 10°, the difference between applying and not applying DDG was 3.0%, 3.2% and 11.7% in FWM, 2.7%, 5.0% and 2.3% in FWHM, 12.2%, 6.3%, and 7.5% in FWTM respectively. It means there is a quantitative correction effect when applying DDG. This shows that the overall experiment has a correction effect when applying DDG.

Key word: PET, Breathing Synchronization System, Motion Artifact, Correction Effect

I. Introduction

Positron emission tomography (PET) can quantitatively measure physiological indicators of the human body by imaging the distribution of biochemical substances in the body. For this reason, it is useful for identifying biochemical or pathological phenomena, diagnosing diseases, determining prognosis after treatment, and planning treatment. Although very useful, PET has the disadvantages of relatively low image resolution and difficulty in assessing anatomical location and relationship to surrounding tissue.

To compensate for these disadvantages, a fusion type PET/CT combining PET and CT has been developed and is currently being actively

used^[1]. Standardized Uptake Value (SUV) is evaluated to assess disease status and tumor uptake and treatment response using 18F-fluorodeoxyglucose (FDG), a glucose derivative, through abnormal uptake by cancer cells. SUV is influenced by patient body shape, blood glucose concentration, tumor size, increased normal tissue uptake, radiopharmaceutical dose and examination time interval, and region of interest (ROI). This phenomenon is used to semi-quantitatively measure the radioactive concentration accumulated in tissues and is currently widely applied in clinical practice^[2-3]. SUV may not be accurately measured due to movement of the diaphragm due to breathing during the examination, and errors may occur in the fusion image of PET and CT, which may cause SUV reading errors and accurate measurement.

With the development of inspection equipment, it has changed to a semiconductor-based collection method, and even in the method of correcting breathing, it is motion-free (data-based gate without a device, DDG), rather than a method of attaching or attaching an external device separately. It is installed as software on the equipment and can be applied practically in the clinical field. DDG is an algorithm that analyzes principal component analysis (PCA)-based data without external equipment to determine the size of respiration and converts it into a respiration waveform. Through this algorithm, it is determined whether or not to correct breathing^[4-6]. Q.Static scan mode (GE Healthcare, Waukesha, WI) is a phase-based gating correction method that extracts a portion of PET data from a stable part of the respiratory cycle. Since a relatively stable breathing area is

obtained, Q. Static scan reduces respiratory motion artifact and creates a corrected image^[7].

In this study, DDG and Q.Static scan modes according to condition changes using a phantom are applied and a comparative experiment is performed to confirm and evaluate the practicality effect.

II. Materials and Methods

1. PET/CT

(1) Basic principle

PET is an imaging method using unstable radioactive isotopes such as ¹⁸F, ¹¹C, ¹³N, and ¹⁵O, because the number of neutrons is relatively small compared to the number of protons in the nucleus. These radioactive isotopes emit a positron when a proton is converted into a neutron in the nucleus. After flying a certain distance, the positrons emitted in this way meet electrons around the nucleus and annihilate, emitting two gamma rays with an energy of 511 keV. At this time, the two gamma rays are emitted in opposite directions of 180° within a very small error range according to the law of conservation of energy and momentum, and PET detects them simultaneously and records the direction and position of the emitted gamma rays^[1].

(2) Radioactive isotopes used in PET/CT

The most widely used radiotracer for PET imaging is ¹⁸F-labeled ¹⁸F-fluorodeoxyglucose(FDG), a glucose analogue. It provides information on abnormal glucose metabolism and is used for diagnosis of various diseases including malignant tumors, epilepsy, and Alzheimer's disease.

Table 1 shows radioactive isotopes that are typically used for PET^[1].

Table 1. Radioactive isotopes used in PET

Nuclide.	HL(Min)	Max energy(MeV)
¹¹ C	20.4	0.96
¹³ N	9.96	1.20
¹⁵ O	2.03	1.74
¹⁸ F	109.7	0.63
⁶⁸ Ge	68.3	1.90
⁸² Rb	1.25	3.40
¹²⁴ I	6000	2.13

2. Artifacts

Artifacts that can be produced during PET/CT include metal artifacts, respiration artifacts, and truncation artifacts. Among them, in the case of breathing, which is one of the purposes of this paper, the difference in position of the liver, an abdominal organ, due to breathing can occur up to 5.5 cm, and even during normal breathing or artificially stopping breathing, the difference is 2.5 cm and 0.9 cm, respectively^[8]. Accordingly, artifacts caused by respiration may be created, and lesions may be distorted or affect reading without being accurately expressed in the portion where the artifacts are created [Figure 1].

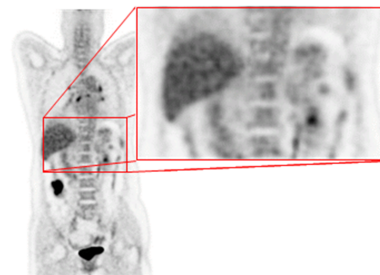


Figure 1. Artifact creation by breathing motion

3. Respiratory correction

As a method of correcting respiration, the Pulmonary toolkit attaches a respiration correction tube to the abdomen and displays the contraction and relaxation of the tube according to respiration as a graph, or the Rpm Respiratory gating system displays the movement of the patient's respiration as a graph to target the patient's abdomen. . The equipment had a correction method using software CTAC shift and an artifact correction method^[9-11]. In this study, artifacts caused by respiratory motion were corrected using MotionFree (Device-less data-driven gated, DDG), a respiratory synchronization system installed in the equipment, and Q.static scan mode without installing such an external device, and its we want to evaluate practicality.

III. research methods

1. Experiment equipment and materials

(1) Phantom

The phantom (National Electrical Manufacturers Association (NEMA) IEC Body Phantom) is in the form of six spheres, each having a volume of 10, 13, 17, 22, 28, and 37 mm. [Figure 2]

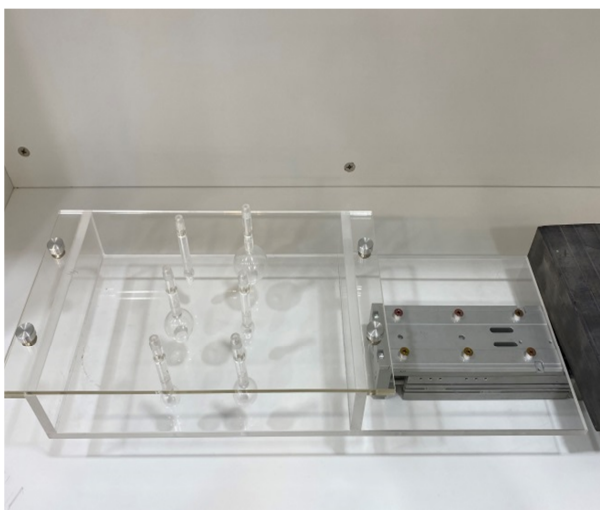


Figure 2. Phantom: NEMA IEC Body Phantom

(2) Position and velocity module

LXSH2BD-50S-M9N2 (SMC, Tokyo, Japan), one of the LX Series models, was used as an electric actuator to adjust the position and speed. The LC6C-220AD (SMC, Tokyo, Japan) used as an electric actuator positioning driver has a built-in pulse control function. Position information can be set up to 28 points, point movement can be controlled by PLC, and it is compatible with electric actuators and 2-phase stepping motors. A PLC (Programmable Logic Controller) is a program-embedded control and monitoring device that stores a program instructing the operation process sequence in the control device and processes and operates according to the program [12].



Figure 3. Position and speed control module

Figure 3 is the actual appearance of the module that controls the position and speed, and as an operating system for controlling it, it has the same functions as Figure 4 based on Windows CE 6.0. Details are as follows [12].

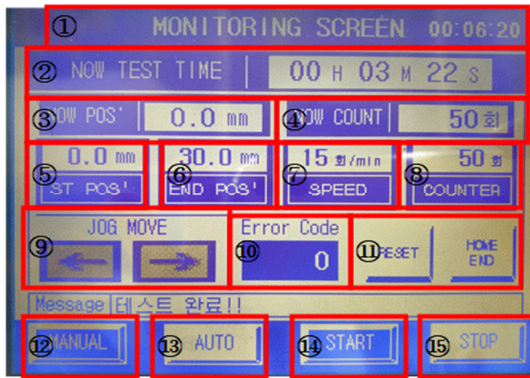


Figure 4. Operation screens such as distance and number of trips, reset, start, etc.

- ① MONITORING SCREEN: When touched, it converts to the MOVING calibration constant value input screen of the device.
- ② NOW TEST TIME: Movement time up to now
- ③ NOW POS' (unit, mm): current position
- ④ NOW COUNT (unit, times): Number of round trips so far
- ⑤ ST POS' (unit, mm): Starting position for round trip (050)
- ⑥ END POS' (unit, times): End position for round trip (0~50)
- ⑦ SPEED (unit, times/min): Setting the number of round trips per minute (0~20)
- ⑧ COUNTER (unit, times): Setting the number of round trips (0~20000 times)
- ⑨ JOG MOVE : JOG can be moved in MANUAL mode
- ⑩ ERROR CODE: Displays the corresponding code when an error occurs
- ⑪ RESET: HOME END RESET, HOME POS': Stopped JOG to POS' 0mm
bring back
- ⑫ MANUAL: Manually move JOG,
- ⑬ AUTO: Move JOG with set value
- ⑭ START: MOVING starts. Available only in AUTO state

⑮ STOP: Stop MOVING

(3) Data Acquisition PET/CT

Discovery MI Generation 2 (GE healthcare, Milwaukee, WI) was used as equipment, and basic information is as follows. [Figure 5, Table 2]



Figure 5. Discovery MI Generation 2 (GE healthcare, Milwaukee, WI, USA)

Table 2. PET/CT basic information

	PET	CT	
Detector type	SiPM	Max scan Field of view	50 cm
Crystal type	LBS	Max. number of row	64 row
Crystal dimensions	3.95×5.3×25 mm	Max. number of slices per gantry rotation	128
Axial FOV	20 cm	Detector size	40 mm
Overlap ratio	23 %	Detector elements	54272
Effective Axial FOV	15.4 cm	Max kVp range	140 kVp
		Max mA range	600 mA

2. Experiment method

(1) Experiment preparation and image acquisition method

18F-fluorodeoxyglucose (FDG) mixed with 37 MBq in 600 cc of physiological saline was dispensed to each sphere and fixed to an electric actuator. The PET condition was set to 1 minute and 30 seconds per bed to apply the same as when examining the patient, and the image was reconstructed by applying the same algorithm. In the case of DDG, when the test starts, the breathing cycle is automatically recognized by movement, and in Q.Static scan mode, the phase offset (the area where data will not be acquired) and the phase width (the area where data will be acquired) are specified. 30% and 50%, respectively, were applied to be the same as the setting applied to the patient. The threshold for determining whether or not to apply DDG was also applied in the same setting as for patients [Figure 6].

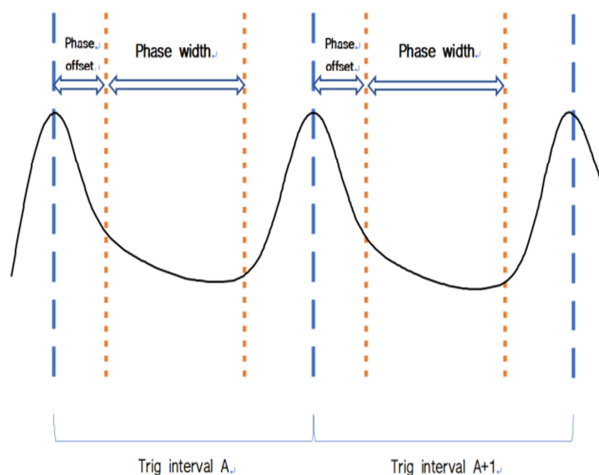


Figure 6. Classification of phase offset and phase width in the respiratory cycle

1) Measurement of the phantom movement distance and movement speed

The phantom movement distance was set to 0 cm, 1 cm, 2 cm, and 3 cm in consideration of the patient's situation, and the number of breaths was fixed at 15. Using a motion detector (Vernier Motion Detector 2), a data acquisition device (Vernier LabPro®), and a personal computer (LABTOP PC), it was confirmed that the correct motion was performed under the set conditions. The motion detector (Vernier Motion Detector 2) has a function of emitting ultrasonic waves from a gold foil ultrasonic transducer and receiving a returning echo. The measurement range of the motion detector is from 15 cm to 6 m, the resolution is ± 1 mm, the frequency is 50 kHz, and the shape of the ultrasonic wave is a cone beam that is 15 to 20° from the central axis. The time for the ultrasonic waves generated from the ultrasonic transducer to move to the breath-simulating motion phantom and return to the ultrasonic transducer was measured and transmitted to a data acquisition device (Vernier LabPro®), and the data were stored in a personal computer to analyze the movement distance and movement speed. [12]

2) Change the travel distance

After fixing the inclination of the electric actuator with the phantom installed at 0°, setting the respiratory rate to 15 times, and adjusting the movement distance to 0 cm, 1 cm, 2 cm, and 3 cm, respectively, the experiment image and DDG without applying DDG were obtained. The images applied and tested were compared respectively.

3) Change the slope

After setting the moving distance of the electric actuator to 1 cm and setting the respiratory rate to 15 as in the previous experiment, experiment without applying DDG by adjusting the inclination to 0°, 2.5°, 5°, and 10° using an electronic goniometer. One image and DDG applied and tested images were

compared [Figure 7].



Figure 7. Phantom before and after gradient adjustment

3. Evaluation method

ImageJ was used for PET/CT image analysis. ImageJ (National Institutes of Health, USA) is a Java-based free program for displaying, analyzing, and processing 8-bit, 16-bit, and 32-bit images. In this paper, the image was analyzed using the area, pixel value, and line plot profile using the Windows platform, Windows 10 OS, and ImageJ 1.8.0.

(1) Changes in SUVmax and SUVmean

Standardized Uptake Values (SUV) is a semi-quantitative index that analyzes the relationship between radioactive uptake in a specific area, such as a tumor, under the assumption that the radionuclide injected into the measurement target is evenly distributed over the entire volume of the measurement target. SUV can be expressed by the equation below.

$$SUV = \frac{\text{radiopharmaceutical concentration } (\frac{kBq}{mL})}{\frac{\text{injected activity (MBq)}}{\text{normalizing factor (BW, BSA, LBM ...)}}}$$

SUVmax means the maximum value of the standard intake coefficient, and SUVmean means the average value of the standard intake coefficient. SUVmax and SUVmean were measured by setting the entire sphere

in the image as a region of interest (ROI) [Figure 8] [13].



Figure 8. SUV measurement method

(2) Changes in area and density of images according to changes in moving distance and inclination.

The data acquisition procedure for comparing the area of an image is ImageJ run -> File > Open -> Image > Type > 8-bit -> Image > Adjust > Threshold -> Plugins – Examples > Image Inventor -> Analyze > Measure -> off It proceeds in the order of line analysis. In order to reduce the error according to the user, the threshold range was set using the Auto function provided by the ImageJ program.

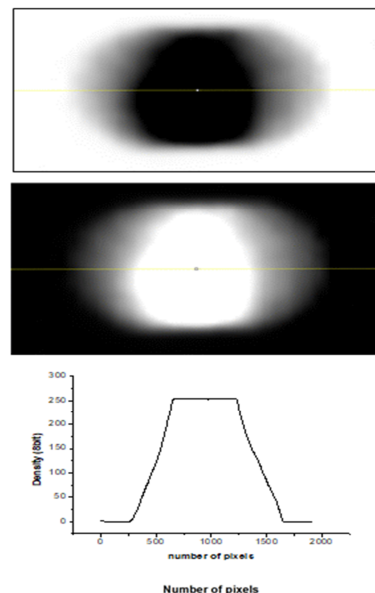


Figure 9. Example of concentration measurement method

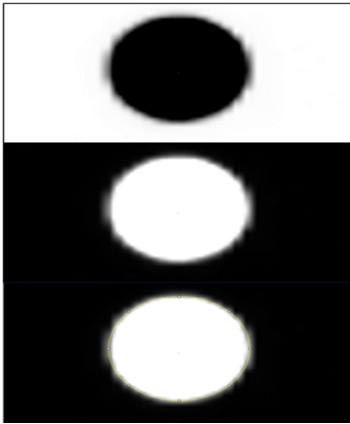


Figure 10. Example of area measurement method

(3) Comparison of full tooth width, half height width, and 1/10 tooth width according to the presence or absence of DDG application

The procedure for acquiring data to compare the full width maximum (FWM), full width half maximum (FWHM), and full width tenth maximum (FWTM) of images is to run ImageJ -> File > Open -> Image > Type > 8-bit -> Plugins - Examples > Image Inventor -> Central Line Settings -> Analyze > Plot Profile -> Off line analysis. For image analysis, full width, half width, and 1/10th width used for radiation energy resolution, pulse duration of signal processing, bandwidth of communication, and apparent size of astronomical objects in astronomy were applied.

The transposition width represents the length of the X-axis at the maximum value of the Y-axis 8-bit image of the line plot profile curve. The half-width represents the length of the X-axis at the middle value (1/2) of the maximum value of the Y-axis 8-bit image of the line plot profile curve. The 1/10 value represents the length of the X-axis at 1/10 of the maximum value of the Y-axis 8-bit image of the line plot profile curve.

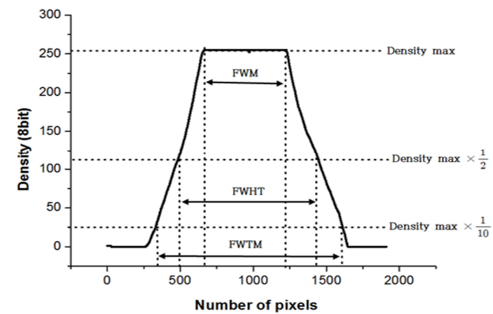


Figure 11. Full Width Maximum, Full Width Half Maximum, Full Width Tenth Maximum

IV. Experiment result

1. Respiratory simulating movement phantom movement distance and movement speed measurement results

When the movement distance of the respiratory simulating motion phantom was set to 1 cm, the range of movement distance was 0 to -10.2 mm with an error of 1.64%, and when the movement distance was set to 2 cm, the range of movement distance was 0.4 to -19.9 mm, an error of 1.77%, and when the movement distance was set to 3 cm, the movement distance range was -0.4 to -29.8 mm and an error of 2.08%.

The reason why the moving distance range appears as a negative number in the experimental results is that the measured distance decreases when the distance between the phantom and the motion monitor is close.

The motion monitor used for the measurement was judged to be an acceptable level considering the error caused by the sampling being set at 0.3 seconds due to the limitation of increasing the sampling speed as a device using ultrasonic waves.

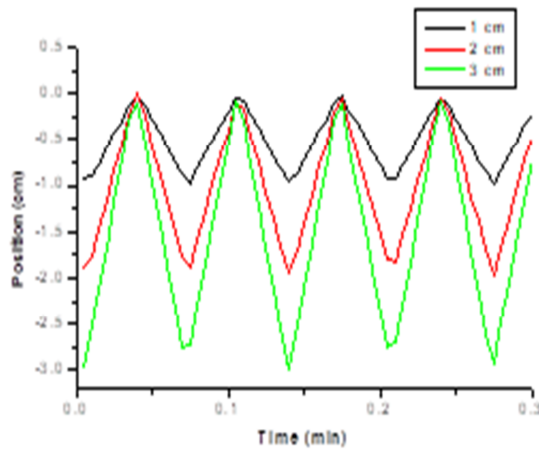


Figure 12. Moving distance range according to the moving distance of the respiratory simulating motion phantom

When the movement distance of the respiratory simulating motion phantom was set to 1 cm, the movement speed range was -32.47 to 32.93 cm/min, and when the movement distance was set to 2 cm, the movement speed range was -63.72 to 64.03 cm/min, and when the movement distance was set to 3 cm, the moving speed range was -91.77 to 92.08 cm/min.

Assuming uniform motion at 15 times per minute and moving distances of 1 cm, 2 cm, and 3 cm, the moving speeds are 26.67 cm/min, 53.33 cm/min, and 80.00 cm/min, respectively, but the respiratory simulation was a stop at the start and end points of the reciprocating motion, and the moving speed at the midpoint corresponded to the fastest region. In the moving distance graph and moving speed graph, it was confirmed that the respiratory simulating motion phantom reflected the set conditions.

2. SUVmax and SUVmean measurement results

(1) Change of movement distance

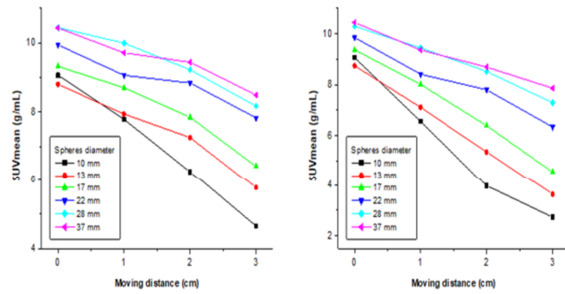
A. SUVmax

In the DDG of SUVmax according to the moving distance, the X-axis moving distance was set to 0cm, 1cm, 2cm, and 3cm, and the Y-axis SUVmax was the maximum value of the standard uptake coefficient. The diameters of the six spheres included in the phantom (National Electrical Manufacturers Association (NEMA) IEC Body Phantom) were 10 mm, 13 mm, 17 mm, 22 mm, 28 mm, and 37 mm, respectively. In SUVmax, the larger the sphere diameter, the smaller the effect of the movement distance, and the smaller the sphere diameter, the larger the effect of the movement distance. The mean and standard deviation of SUVmax at the moving distances of 0 cm, 1 cm, 2 cm, and 3 cm were 13.03 ± 0.39 , 11.95 ± 1.81 , 10.25 ± 3.64 , and 8.07 ± 3.82 in the DDG unapplied image, respectively. In the case of motion, the image DDG applied had a higher average SUVmax than the image DDG unapplied, and the standard deviation was smaller, indicating that there was a correction effect.

A correction effect of SUVmax according to the moving distance. the X-axis is the diameter of the phantom sphere, which is 10 mm, 13 mm, 17 mm, 22 mm, 28 mm, and 37 mm, respectively, and the SUVmax on the Y-axis is the maximum standard uptake coefficient. Based on the moving distance, it was found that the average SUVmax moving distance was improved in the image to which DDG was applied compared to the image to which DDG was not applied. Also, based on the diameter of the phantom sphere, it was found that the average

SUVmax of the DDG-applied image was improved compared to the DDG-unapplied image.

B. SUVmean



a. SUVmean of DDG applied image. b. SUVmean of DDG non-applied image.

Figure 13. SUVmean (DDG applied and DDG unapplied) according to the moving distance

Figure 13-a is the DDG application graph of SUVmean according to the moving distance, and Figure 13-b is the DDG unapplied graph. In DDG of SUVmean according to moving distance, the moving distance was set as 0 cm, 1 cm, 2 cm, and 3 cm on the X-axis, and SUVmean on the Y-axis is the average value of standard uptake coefficients. As for SUVmean, the larger the diameter of the sphere, the smaller the effect of the distance traveled, and the smaller the diameter of the sphere, the greater the effect of the distance traveled. As the moving distance increases, the SUVmean decreases regardless of the size of the sphere. The mean and standard deviation of SUVmean at the moving distances of 0 cm, 1 cm, 2 cm, and 3 cm were 9.67 ± 0.71 , 8.87 ± 0.90 , 8.15 ± 1.24 , and 6.89 ± 1.52 , respectively, in the DDG-applied images. The images DDG unapplied were 9.63 ± 0.68 , 8.15 ± 1.17 , 6.79 ± 1.89 , and 5.40 ± 2.07 , respectively. In the case of motion, the average of SUVmean was higher in the image to which DDG was applied than in the image to which DDG was not applied, and the standard deviation was small, indicating that there was a correction effect.

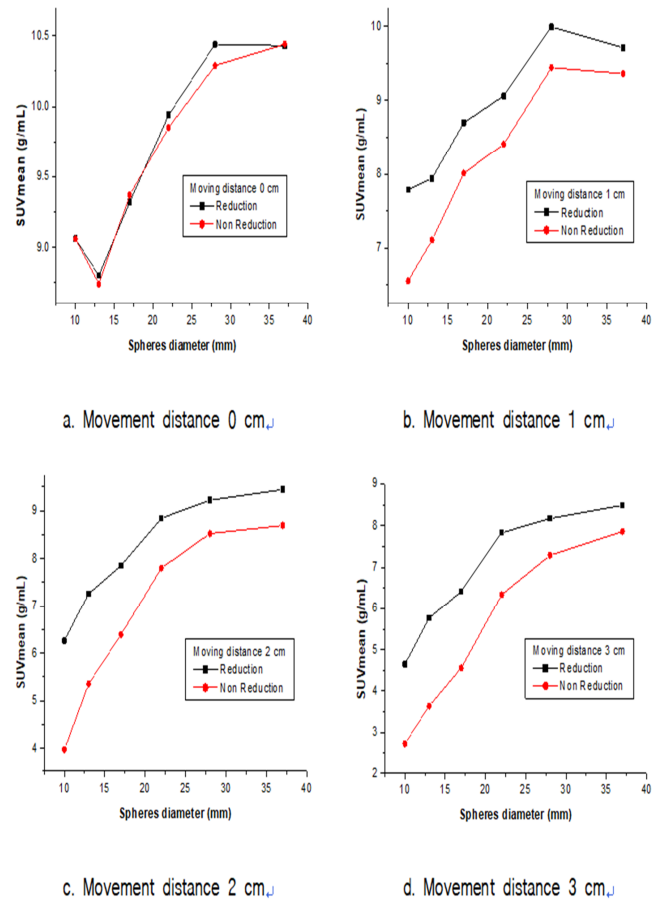
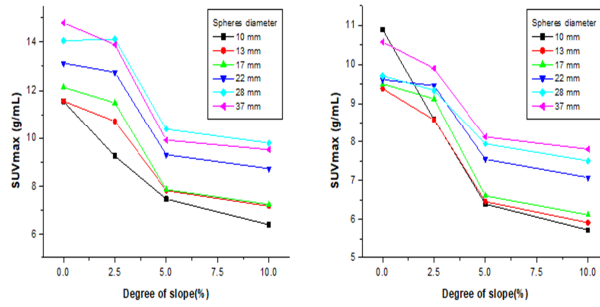


Figure 14. SUVmean correction effect according to movement distance

A SUVmean is correction effect according to movement distance. On the X-axis, the diameters of the phantom spheres were 10 mm, 13 mm, 17 mm, 22 mm, 28 mm, and 37 mm, respectively, and the SUVmean on the Y-axis is the mean value of the standard uptake coefficient. Based on the moving distance, it was found that the average SUVmean moving distance of the DDG-applied image was improved compared to the DDG-unapplied image. Based on the diameter of the phantom sphere, it was found that the average SUVmean of the DDG-applied image was improved compared to the DDG-unapplied image.

(2) gradient change

A. SUVmax



a. SUVmax of DDG applied image b. SUVmax of DDG unapplied image

Figure 15. SUVmax according to gradient(DDG applied and DDG unapplied images)

Figure 15-a is a graph of SUVmax applied DDG according to the gradient, and Figure 15-b is a graph of unapplied DDG. In the figure, the X-axis is the gradient, 0°, 2.5°, 5°, and 10°, and the Y-axis is the maximum value of the standard uptake coefficient of SUVmax. The diameters of the six spheres in the phantom were 10 mm, 13 mm, 17 mm, 22 mm, 28 mm, and 37 mm, respectively, as in the moving distance change experiment. It was found that as the gradient increases, SUVmax decreases regardless of the size of the sphere.

The mean and standard deviation of SUVmax at gradients of 0°, 2.5°, 5°, and 10° were 12.87±1.35, 12.04±1.90, 8.79±1.23, and 8.14±1.40 in the image to which DDG was applied, respectively, in the image of DDG unapplied, respectively which were 9.94±0.63, 9.17±0.52, 7.18±0.79, and 6.70±0.89. In the case of motion, it was found that the standard deviation of the DDG-applied image was larger than that of the non-DDG-applied image. However, it was found that the average of SUVmax was higher and

there was a correction effect.

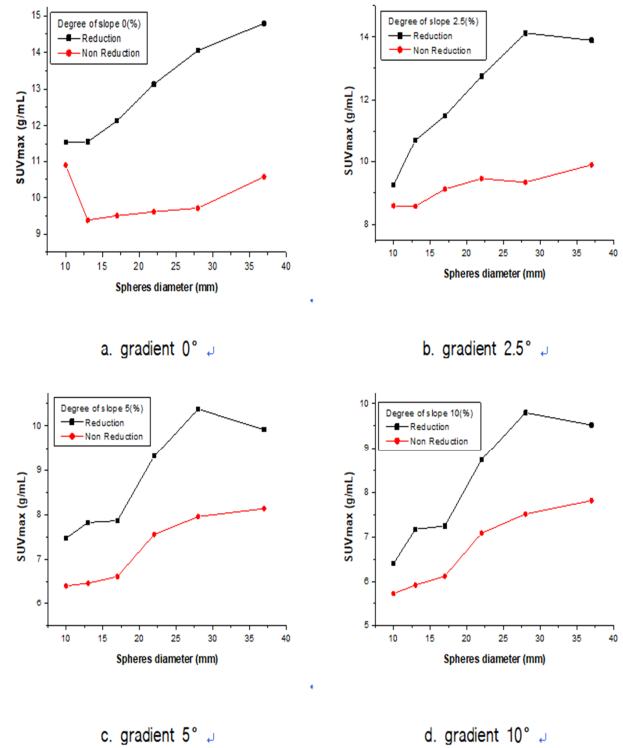


Figure 16. SUVmax correction effect according to the gradients

Figure 16 is a graph of the correction effect of SUVmax according to the gradients. In the figure, the X-axis is the diameter of the phantom sphere, which is 10 mm, 13 mm, 17 mm, 22 mm, 28 mm, and 37 mm, respectively, and the SUVmax on the Y-axis is the maximum standard uptake coefficient. It was found that the image to which DDG was applied improved the average SUVmax by 2.93, 2.87, 1.61, and 1.45 at inclinations of 0°, 2.5°, 5°, and 10°, respectively, compared to the image of DDG-unapplied. It was found that the average SUVmax was improved in the image to which DDG was applied compared to the image to which DDG was not applied.

B. SUVmean

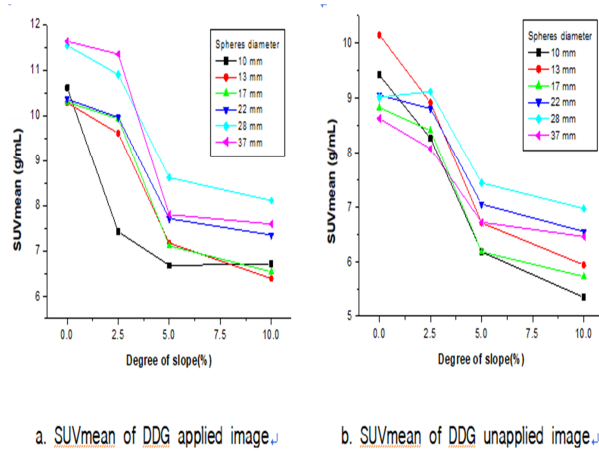


Figure 17. SUVmean according to gradient(DDG applied and DDG unapplied images)

Figure 17 “a” is the DDG applied graph of SUVmean according to the gradients, and Figure 17 “b” is the DDG unapplied graph. The X-axis is the gradient, and it was set at 0°, 2.5°, 5°, and 10°, and the SUVmean of the Y-axis is the average value of the standard uptake coefficient. The diameters of the six spheres in the phantom were 10 mm, 13 mm, 17 mm, 22 mm, 28 mm, and 37 mm, respectively. As the gradient increased, the SUVmean decreased regardless of the sphere size. The mean and standard deviation of SUVmean at gradients of 0°, 2.5°, 5°, and 10° were 10.80±0.63, 9.87±1.37, 7.53±0.68, and 7.13±0.68 in the DDG applied image, respectively. It was 9.19±0.54, 8.60±0.41, 6.72±0.49, and 6.18±0.60, respectively, in the image of DDG unapplied. In the case of motion, the standard deviation of the image applied DDG was higher than the image unapplied DDG, but the average of SUVmean was higher, indicating that there was a correction effect.

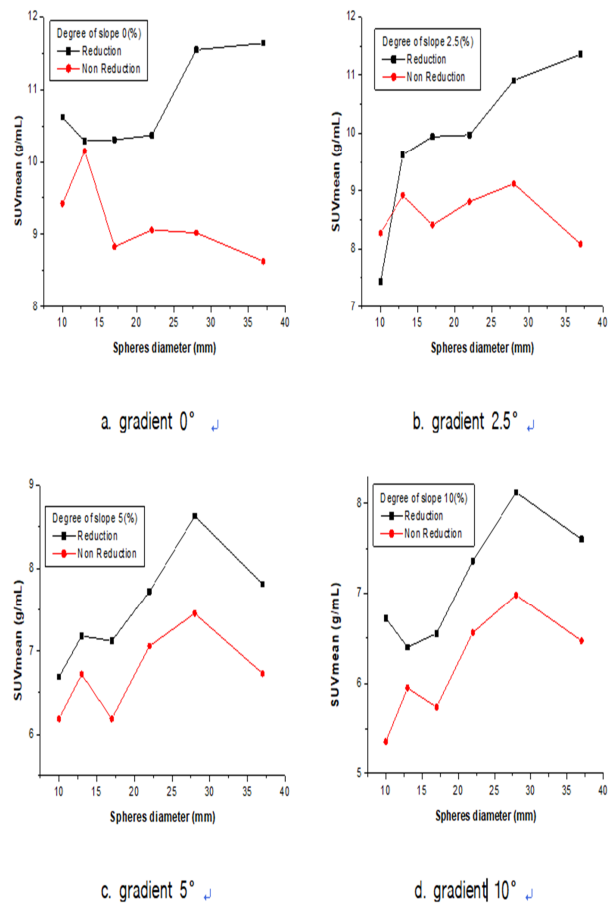


Figure 18. SUVmean correction effect according to the gradients

Figure 18 is a graph of the correction effect of SUVmean according to the gradients. The X-axis was the diameter of the phantom sphere, 10 mm, 13 mm, 17 mm, 22 mm, 28 mm, and 37 mm, respectively. SUVmean on the Y-axis is the average value of standard uptake coefficients. When the gradient was the criterion, the image of applied DDG improved the average SUVmean by 1.61, 1.27, 0.80, and 0.95 at gradients of 0°, 2.5°, 5°, and 10°, respectively, compared to images of unapplied DDG. When the diameter of the phantom was the criterion, on the image of DDG applied has a SUVmean of 0.56, 0.44, 1.19, 0.98, It was found to improve 1.66 and 2.13.

3. Changes in the area and density of images according to the change in moving distance and gradient

A. Change in moving distance

1) Visual comparison

In the visual comparison of the moving distance change images with and without DDG application, the hot cell boundary of the image changed indistinctly as the moving distance increased to 0 cm, 1 cm, 2 cm, and 3 cm regardless of whether or not DDG was applied. In addition, when DDG was applied, it was qualitatively confirmed that there was a correction effect at all of the movement distances of 1 cm, 2 cm, and 3 cm. It was found that the correction effect of DDG increased as the moving distance increased.

2) Area ratio

In the 37mm sphere, the ratio of hot cell area according to the movement distance increased by 7%, 18%, and 30% at movement distances of 1cm, 2cm, and 3cm compared to the reference image (movement distance of 0 cm) when DDG was not applied. And, when DDG was applied, the movement distance compared to the reference image (movement distance 0 cm) increased by 2%, 6%, and 12% at 1cm, 2cm, and 3cm, respectively. The difference between when DDG was applied and when it was not applied was 5%, 12%, and 18% at 1 cm, 2 cm, and 3 cm, respectively, which means the quantitative correction effect when DDG was applied, and the standard It was corrected toward closer to the ten-pixel area of the image.

3) Average concentration ratio

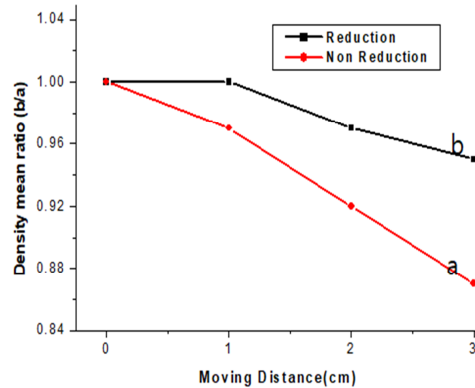


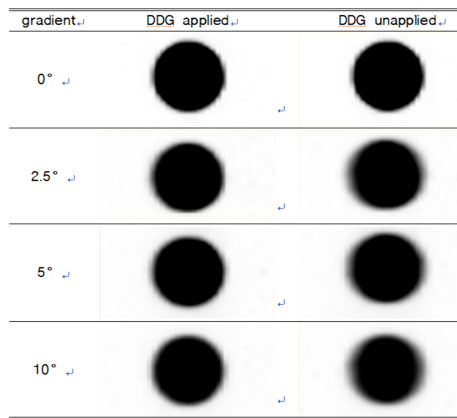
Figure 19. Ratio of hot cell average density by moving distance on a 37 mm sphere.

In Figure 19, the X-axis is the movement distance, 0 cm, 1 cm, 2 cm, 3 cm, and the Y-axis is the average density ratio, “a” is the average density of hot cells in the reference image, “b” is 0 cm, it means the average concentration at 1 cm, 2 cm, and 3 cm. The average density ratio of the comparison image compared to the reference image with a moving distance of 0 cm decreased by 3%, 8%, and 13% at moving distances of 1 cm, 2 cm, and 3 cm, respectively, when DDG was not applied, and when DDG was applied the moving distance decreased by 0%, 3%, and 5% at 1 cm, 2 cm, and 3 cm, respectively. The difference between when DDG was applied and when it was not applied was 3%, 6%, and 8% at 1 cm, 2 cm, and 3 cm, respectively. This means the quantitative correction effect when using the DDG correction program, and it was corrected to be close to the average density of the reference image.

B. Gradient change

1) Visual comparison

Table 3. Visual comparison of gradient change images with and without DDG application



As shown in Table 3, when the images of gradient changes with and without DDG application were visually compared, the borderline of the image changed indistinctly as the gradient increased to 0°, 2.5°, 5°, and 10° in both methods. When DDG was applied, it was qualitatively confirmed that there was a correction effect at all moving distances of 2.5°, 5°, and 10°. The correction effect of applying DDG was found to be greater as the gradient increased.

2) Area ratio

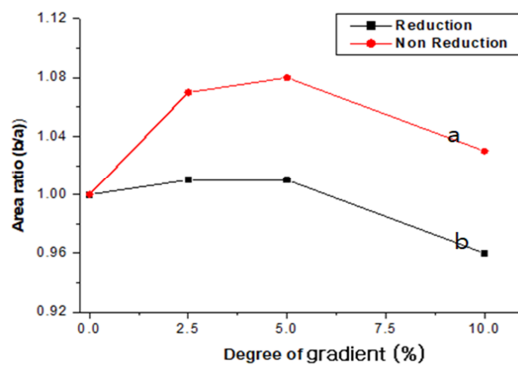


Figure 20. Hot cell area ratio according to gradient on a 37 mm sphere

The X-axis in Figure 20 is the gradient, 0°, 2.5°, 5°, 10°, and the Y-axis is the area ratio. "a" means the area of hot cell of the reference image. "b" means the area of hot cell at 0°, 2.5°, 5°, and 10°. When DDG was not applied, the area ratio of the reference image with an inclination of 0° and the comparison image with an inclination of 2.5°, 5°, and 10° increased by 7%, 8%, and 3%, respectively. And when DDG was

applied, the gradient increased by 1% and 1% at 2.5° and 5°, respectively, and decreased by 4% at 10°. The difference between when DDG was applied and when it was not applied was 6%, 7%, and 7% at 2.5°, 5°, and 10°, respectively. This means the quantitative correction effect when DDG is applied. It was corrected to the side close to the hot cell area of the reference image. However, at 10°, the correction was excessive, resulting in 4% smaller than the reference image.

3) Average concentration ratio

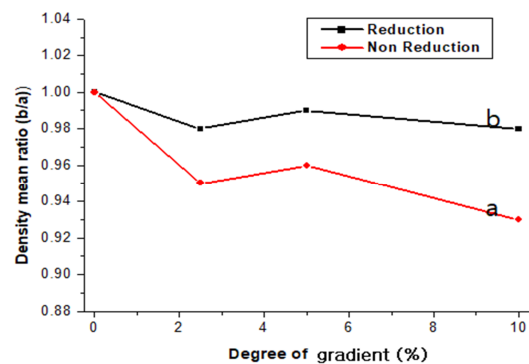


Figure 21. Hot cell average density ratio according to gradient on a 37 mm sphere

The X-axis in Figure 21 is the gradient 0°, 2.5°, 5°, 10°, and the Y-axis is the average density ratio. "a" means the average density of hot cell of the reference image, and "b" means the average density of hot cell at 0°, 2.5°, 5°, and 10°. When DDG was not applied, 5%, 4%, and 7% decreased in the reference image with 0° gradient and the 2.5°, 5°, and 10° images, respectively. When DDG was applied, the gradient decreased by 2%, 1%, and 2% at 2.5°, 5°, and 10°, respectively. The difference between when DDG was applied and when it was not applied was 3%, 4%, and 5% at 2.5°, 5°, and 10°, respectively. This means the quantitative correction effect when DDG was applied, and it was corrected to be close to the average density of hot cell of the reference image.

4. Comparison of FWM, FWHM, and FWTM with and without DDG application

A. Change in moving distance

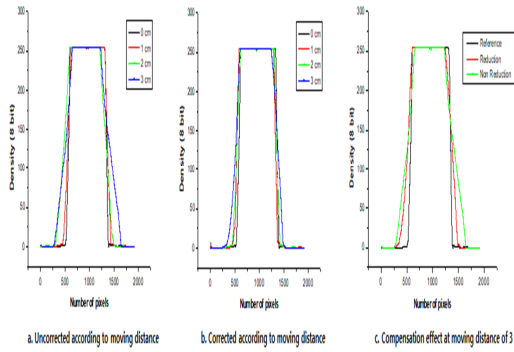


Figure 22. Profile curve according moving distance

Figure 22 shows the density of the area for each moving distance using ImageJ, and was drawn based on the experimentally acquired images according to the moving distance. Figure 22 “a” is the density graph without applying DDG according to the moving distance, and 21 “b” is the density graph with the application of DDG according to the moving distance. Figure 22 “c” is a graph comparing an image with a moving distance of 3 cm to an image with a moving distance of 0 cm. Through this, it was confirmed that the images were widely distributed compared to the image when the moving distance was 0 cm, which is the reference image.

1) Comparison of FWM ratio

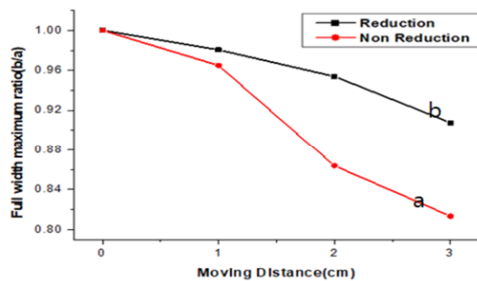


Figure 23. Comparison of FWM ratio change with and without DDG application

In Figure 23, the X-axis represents the moving distance at 0 cm, 1 cm, 2 cm, and 3 cm, and the Y-axis represents the FWM ratio. “a” means the FWM of the hot cell of the reference image, and “b” means the FWM of the hot cell at 0 cm, 1 cm, 2 cm, and 3 cm. When DDG was not applied, as a result of comparing the reference image with a moving distance of 0 cm and the images at moving distances of 1 cm, 2 cm, and 3 cm, the reduction was reduced by 3.5%, 13.6%, and 18.7%, respectively. And when DDG was applied, the movement distance decreased by 2%, 4.6%, and 9.2% at 1 cm, 2 cm, and 3 cm, respectively. The difference between when DDG was applied and when it was not applied was 1.6%, 9%, and 9.4% at 1 cm, 2 cm, and 3 cm, respectively. This means the quantitative correction effect when DDG is applied, and it was corrected to the side close to the FWM of the hot cell of the reference image. The transposition width of all images decreased when DDG was applied and when it was not applied. This is because the hot cell of the moving image appear smaller than they actually are.

2) Comparison of FWHM ratio

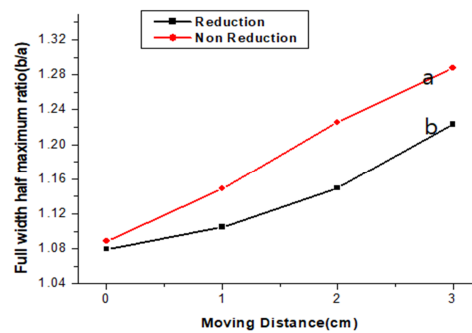


Figure 24. Comparison of FWHM ratio change with and without DDG application

The X-axis in Figure 24 is the moving distance, 0 cm, 1 cm, 2 cm, and 3 cm, and the Y-axis is the FWHM

ratio. “a” means a FWHM of a hot cell of the reference image, and “b” means a FWHM of a hot cell in 0 cm, 1 cm, 2 cm, and 3 cm. When DDG was not applied, the FWHM ratio increased to 14.9%, 22.6%, and 28.8% in the reference image with a moving distance of 0 cm and the comparison images with moving distances of 1 cm, 2 cm, and 3 cm. When DDG was applied, the moving distance increased by 10.5%, 14.9%, and 22.3% in 1 cm, 2 cm, and 3 cm, respectively. The difference between when DDG was applied and when it was not applied was 4.4%, 7.6%, and 6.4% at 1 cm, 2 cm, and 3 cm, respectively. This means the quantitative correction effect when DDG is applied and means that it is corrected to the side close to the FWHM of the hot cells of the reference image.

The FWHM of the image increased both when DDG was applied and when it was not applied. The reason is that the hot cells of the moving image are magnified more than they actually are.

3) Comparison of FWTM ratio

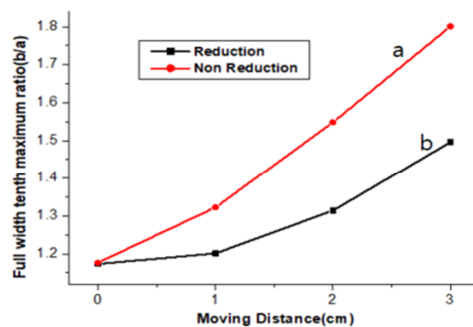


Figure 25. Comparison of FWTM ratio change with and without DDG application

The X-axis in Figure 25 is the moving distance in 0 cm, 1 cm, 2 cm, and 3 cm, and the Y-axis is the FWTM ratio. “a” means the hot cell FWTM of the reference image, and “b” means the FWTM of the hot cell at 0 cm, 1 cm, 2 cm, and 3 cm. When DDG

was not applied, the FWTM ratio increased by 32.3%, 54.8%, and 80.1% in the reference image with a moving distance of 0 cm and the comparative images with moving distances of 1 cm, 2 cm, and 3 cm, respectively. When DDG was applied, it increased by 20.1%, 31.4%, and 49.6% in images of 1 cm, 2 cm, and 3 cm, respectively. The difference between when DDG was applied and when it was not applied was 12.1%, 23.4%, and 30.5% at 1 cm, 2 cm, and 3 cm, respectively. This means the quantitative correction effect when DDG is applied and means that it is corrected to the side close to the FWTM of the hot cell of the reference image. The FWTM of the image increased both when DDG was applied and when it was not applied. The reason is that the hot cell of the moving image is enlarged more than the real one.

B. Gradient change

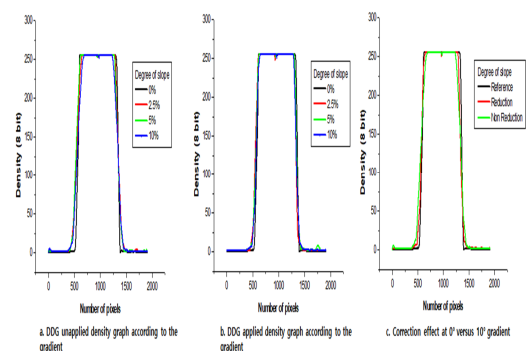


Figure 26. Profile curve according to gradient

In Figure 26, "a" is the density graph according to the gradient when DDG is not applied, and "b" is the density graph when DDG is applied. "c" is a graph comparing a reference image with an gradient of 0° and a comparison image with an gradient of 10° when DDG is applied. In the "c" graph, it was found that when DDG was applied, it became closer to the reference image.

1) Comparison of FWM ratio

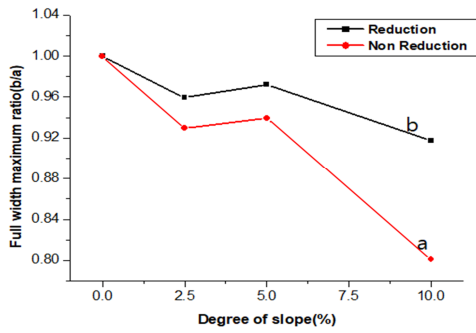


Figure 27. Comparison of FWM of gradient change images with and without DDG application

The X-axis in Figure 27 is the gradient 0°, 2.5°, 5°, 10°, and the Y-axis is the FWM ratio. “a” means the hot cell FWM of the reference image, and “b” means the hot cell FWM at 0°, 2.5°, 5°, and 10°. When DDG was not applied, the FWM ratio decreased by 7.0%, 6.0%, and 19.9% in the reference image with an gradient of 0° and the comparison image with an gradient of 2.5°, 5°, and 10°, respectively. When DDG was applied, the FWM ratio decreased by 4.1%, 2.8%, and 8.2%, respectively, in the 2.5°, 5°, and 10° comparison images. The difference between applying and not applying DDG was 3.0%, 3.2%, and 11.7% at 2.5°, 5°, and 10°, respectively. This means the quantitative correction effect when DDG is applied and means that it is corrected closer to the hot cell FWM of the reference image. The FWM of the image decreased both when DDG was applied and when it was not applied. The reason is that the hot cell of the moving image are reduced than they actually are.

2) Comparison of FWHM ratio

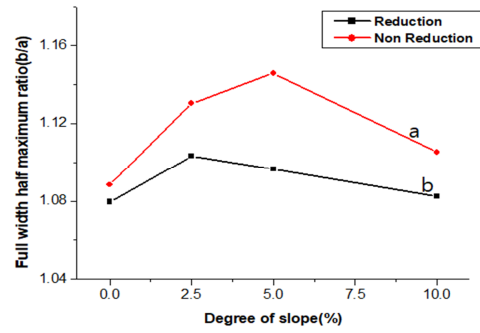


Figure 28. Comparison of FWHM of gradient change images with and without DDG application

The X-axis in Figure 28 is the inclination of 0°, 2.5°, 5°, and 10°, and the Y-axis is the FWHM ratio. “a” means the hot cell FWHM of the reference image, and “b” means the hot cell FWHM at 0°, 2.5°, 5°, and 10°. When DDG was not applied, the FWHM ratio increased by 13.0%, 14.6%, and 10.5% in the reference image with an inclination of 0° and the comparison image with an inclination of 2.5°, 5°, and 10°, respectively. When DDG was applied, it increased by 10.3, 9.6%, and 8.2%, respectively, in comparison images with slopes of 2.5°, 5°, and 10°. The difference between applying and not applying DDG was 2.7%, 5.0%, and 2.3% at 2.5°, 5°, and 10°, respectively. This means that the quantitative correction effect when DDG was applied and the correction was made to the side close to the hot cell FWHM of the reference image. The FWHM of the image decreased both when DDG was applied and when it was not applied.

3) Comparison of FWTM ratio

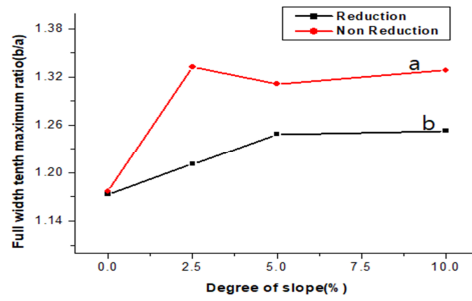


Figure 29. Comparison of FWTM of gradient change images with and without DDG application

The X-axis of Figure 29 is the inclination of 0° , 2.5° , 5° , and 10° , and the Y-axis is the FWTM ratio. “a” means the hot cell FWTM of the reference image, and “b” means the hot cell FWTM at 0° , 2.5° , 5° , and 10° . When DDG was not applied, it increased by 33.2%, 31.1%, and 32.8% in the reference image with an inclination of 0° and the comparison image with an inclination of 2.5° , 5° , and 10° , respectively. When DDG was applied, in comparison images with slopes of 2.5° , 5° , and 10° , increased by 21.1%, 24.9%, and 25.3%, respectively. The difference between applying and not applying DDG was 12.2%, 6.3%, and 7.5% at 2.5° , 5° , and 10° , respectively. This means the quantitative correction effect when DDG is applied and means that it is corrected closer to the hot cell FWTM of the reference image. The FWTM of the image decreased both when DDG was applied and when it was not applied. The reason is that the hot cell of the moving image are magnified more than they actually are.

V. Review

The average correction effect according to the moving distance through the experiment was as follows.

1. As for the correction effect of the moving distance criterion, SUVmax was improved by 1.92, 2.48, 3.23, and 3.00 when DDG was applied, and SUVmean was

improved by 0.04, 0.72, 1.36, and 1.49, respectively. 2. The correction effect based on the phantom sphere diameter improved SUVmax by 2.37, 2.02, 1.44, 1.20, 0.42, 0.52, and SUVmean by 1.36, 1.23, 0.99, 0.82, 0.57, and 0.43, respectively, when DDG was applied.

The average correction effect according to the gradient was as follows.

1. The correction effect based on the slope improved SUVmax by 2.93, 2.87, 1.61, 1.45, and SUVmean by 1.61, 1.27, 0.80, and 0.95, respectively, when DDG was applied.

2. The correction effect based on the phantom sphere diameter was 0.77, 1.73, 1.84, 2.56, and 3.46 respectively for SUVmax when DDG was applied. 2.93 and SUVmean improved by 0.56, 0.44, 1.19, 0.98, 1.66, and 2.13, respectively.

In the visual comparison according to the change in the moving distance and the gradient, the correction effect of DDG increased as the moving distance increased and the gradient increased. In the case of the area ratio, the difference between the reference image with the moving distance of 0 cm and DDG applied and not applied was 5%, 12%, and 18%, respectively. In the reference image with an gradient of 0° and the comparison image with an gradient of 2.5° , 5° , and 10° , the difference between applying and not applying DDG was 6%, 7%, and 7%, respectively. It was confirmed that there was a correction effect.

In the case of the average density ratio, the difference between applying and not applying DDG was 3%, 6%, and 8%, respectively, in the reference image and comparison image with a moving distance of 0 cm. In the reference image and comparative image with a gradient of 0° , the average density ratio showed a

difference of 3%, 4%, and 5% with and without DDG application, respectively.

When comparing FWM, FWHM, and FWTM, the difference between applying and not applying DDG according to the change in moving distance was 1.6%, 9%, and 9.4% in FWM, 4.4%, 7.6%, and 6.4% in FWHM, and 12.1%, 23.4% and 30.5% in FWTM, respectively. In the gradient change, the difference between applying and not applying DDG was 3.0%, 3.2%, and 11.7% in FWM, 2.7%, 5.0%, and 2.3% in FWHM, and 12.2%, 6.3%, and 7.5% in FWTM.

This means the quantitative correction effect when DDG is applied. As a result, it was found that there was a correction effect in the overall experiment according to the change of the moving distance and gradient when DDG was applied. However, this experiment result this is not a direct application to this the patient, but an experiment using a phantom, and even if a three-dimensional motion is created by combining with an electric actuator by tilting, it is different from the actual respiration movement of the patient. the error should be taken into account. In addition, since the waveform of the motion of the electric actuator may be different from the waveform of respiration, the resulting error should be considered. It has been reported that it is appropriate to apply the phase offset and phase width adjustment ranges of 30% to 50% in Q.Static scan mode, but this also varies depending on the degree of movement for each patient, so errors in range adjustment should also be considered^[14].

In addition, when DDG is applied by setting the range of phase width to 50% using Q.Static scan mode, it is pointed out as an inevitable disadvantage that the inspection time is doubled compared to the existing inspection time.

VI. conclusion

During PET/CT examination, artifacts due to respiration inevitably occur, and if a lesion is located in the lower lung or upper liver, the artifact due to respiration must be corrected for accurate measurement and examination of SUV or reading error. DDG and Q.static scan mode were used among methods to reduce artifacts caused by respiration, and the movement of respiration was simulated using a phantom. Through the results of the experiment according to the change of the moving distance and the gradient, it was found that when DDG was applied to artifacts caused by motion, there was a correction effect more than when DDG was not applied.

In addition, because it does not require the installation of a separate external device to correct respiration, improved images can be obtained more simply. As a result, it is possible to reduce time consumption examination time delay due to the installation of an external device, and a reduction in radiation exposure of the operator can be expected. In this paper, a method to improve the quantitative PET image quality by applying DDG and Q.static scan mode was proposed.

Competing interests

The authors declare that there are no competing interests.

[Reference]

- [1] C. S. Ko, *Nuclear Medicine* (2008)
- [2] Czernin, Johannes, Martin Allen-Auerbach, and Heinrich R. Schelbert. "*Improvements in cancer staging with PET/CT: literature-based evidence as of September 2006.*" *Journal of Nuclear Medicine* 48.1 suppl (2007): 78S-88S. PMID:17204723

- [3] Weber, Wolfgang A. "**Positron emission tomography as an imaging biomarker.**" *Journal of Clinical Oncology* 24.20 (2006): 3282-3292. <https://doi.org/10.1200/JOC.2006.06.6068>
- [4] Walker, Matthew D., Kevin M. Bradley, and Daniel R. McGowan. "**Evaluation of principal component analysis-based data-driven respiratory gating for positron emission tomography.**" *The British journal of radiology* 91.1085 (2018): 20170793. <https://doi.org/10.1259/bjr.20170793>
- [5] Walker, Matthew D., et al. "**Evaluation of data-driven respiratory gating waveforms for clinical PET imaging.**" *EJNMMI research* 9.1 (2019): 1-10. <https://doi.org/10.1186/s13550-018-0470-9>
- [6] THIELEMANS, Kris, et al. "**Device-less gating for PET/CT using PCA**" In: 2011 IEEE Nuclear Science Symposium Conference Record. IEEE, (2011) p. 3904-3910. <https://doi.org/10.1109/NSSMIC.2011.6153742>
- [7] Chen, Yi-Lun, et al. "**Evaluation of PET List Data-driven Gated Motion Correction Technique Applied in Lung Tumors.**", *J. of Medical and Biological Engineering* (2002) Vol. 42, p. 382–387. <https://doi.org/10.1007/s40846-022-00719-2>
- [8] I. Suramo, M. Paivansalo, V. Myllyla, "**Cranio-caudal movements of the liver, pancreas and kidneys in respiration**", *Acta radiologica.: Diagnosis*, (1984) Vol. 25, No. 2, pp. 129-131. <https://doi.org/10.1177/028418518402500208>
- [9] Kim, Ki-Jin, Seok-Hwan Bae, and Ga-Jung Kim. "**Study on the Usefulness of respiration compensation PET/CT.**" *Journal of the Korea Academia-Industrial cooperation Society* (2011) Vol. 12, pp. 2209-2213. <https://doi.org/10.5762/KAIS.2011.12.5.2209>
- [10] Kim, Jin-Young, et al. "**The Research of Comparison Evaluation on the Decline in Artifact Using Respiratory Gating System in PET-CT.**" *The Korean Journal of Nuclear Medicine Technology* (2015) Vol. 19, pp. 63-67. <https://koreascience.kr/article/JAKO201505042695100.kr&sa=U>
- [11] Ham, Jun Cheol, et al. "**Usefulness of CTAC Shift Revision Method of Artifact by Diaphragm in PET/CT.**" *The Korean Journal of Nuclear Medicine Technology* (2013) Vol. 17, pp. 71-75. [https://koreascience.kr/article/JAKO201328635215617.pageDiaphragm in PET/CT](https://koreascience.kr/article/JAKO201328635215617.pageDiaphragm%20in%20PET/CT)
- [12] Jin, Gye-Hwan. "**Defining the Tumour and Gross Tumor Volume using PET/CT: Simulation using Moving Phantom.**" *Journal of the Korean Society of Radiology* (2021) Vol. 15, pp. 935-942 <https://doi.org/10.7742/jksr.2021.15.7.935>
- [13] H. H. Park, D. S. Park, D. C. Kweon, S. B. Lee, K. B. Oh, J. D. Lee, G. H. Jin, "**Inter-comparison of 18F-FDG PET/CT standardized uptake values in Korea**", *Applied Radiation and Isotopes* (2011) Vol. 69, No. 1, pp. 241-246,. <https://doi.org/10.1016/j.apradiso.2010.09.011>
- [14] Meier, Joseph, and Osama Mawlawi. "**Impact of personalized selection of Quiescent phase gating parameters with Q. Static PET/CT imaging.**", *JNM* (2018) Vol. 59, (supplement 1) 1714, [Google Scholar](https://doi.org/10.1016/j.jnm.2018.09.011)